Supporting Information

Elbaum-Garfinkle et al. 10.1073/pnas.1504822112

SI Text

Methods in Detail.

Strain handling and RNAi. All strains were raised at 20 °C unless otherwise indicated and maintained as described previously (1). Living progeny and embryonic lethality were scored using differential interference contrast microscopy. Bristol N2 was used as the *C. elegans* WT strain.

Feeding RNAi was conducted as described previously (2). As a negative control, young adult hermaphrodites were fed with bacteria containing empty pL4440 vector. For *laf-1(RNAi)*, worms were fed a construct targeting nucleotides −35 to 1,338 of *laf-1* mRNA. Every 12 h, exposed mothers were moved to a fresh plate for 60 h in total. After an additional 24 h, plates were screened for living progeny and unhatched embryos. For immunocytochemistry, L4 worms were exposed to RNAi feeding bacteria for 36 h before further processing.

LAF-1 antibody and immunodetection. To examine LAF-1expression and localization, a monoclonal mouse antibody (moBW75) was raised against an MBP-full-length protein fusion and used in a final dilution of 100 ng/mL. Western blot analysis (Fig. S1) of protein extract was performed on 25 gravid hermaphrodites boiled in SDS sample buffer. An HRP-conjugated donkey anti-mouse IgG (Jackson Labs) diluted 1:80,000 was used as a secondary antibody and visualized using the ECL Western blotting detection kit (Amersham). For immunocytochemistry, embryos were freeze-cracked on poly-L-lysine–coated glass slides and fixed in dry ice-cooled methanol and acetone, 5 min each. Samples were probed overnight with antibodies against LAF-1 (1 ng/mL), PGL-1 (3), or PIE-1 (4). Fluorescent dye-coupled secondary antibodies (Jackson Laboratories) were used in a dilution of 1:2,000, and chromatin was visualized with DAPI. Samples were imaged on a Zeiss LSM700 confocal microscope or a Zeiss Imager Z1 equipped with an AxiocamMRm (Zeiss) and analyzed with FIJI (ImageJ) or AxioVision (Zeiss) and processed in Photoshop CS5.1 (Adobe).

Determination of in vivo LAF-1 concentration. LAF-1::GFP concentration in the P lineage cytoplasm was quantified through use of a fluorescence intensity vs. concentration calibration curve generated from a LAF-1::GFP construct expressed in insect cells (see below) and diluted in PBS. Images of embryos at the four-cell stage were taken using a Zeiss inverted microscope equipped with a Yokogawa CSU-X10 confocal spinning disk and 100× objective. Background intensity from autofluorescence in N2 worms were subtracted from the raw intensity before conversion.

Molecular cloning. All molecular subcloning steps were performed using *Escherichia coli* strain DH5α following standard molecular cloning protocols. The LAF-1 gene was codon optimized for *E. coli*, synthesized by GenScript, and inserted in a pET28a backbone with a C-terminal 6×-His tag. The amino acid sequence of LAF-1 is listed below. The following deletion mutants were generated: C-term deletion (M1-F647); N-term deletion (G168-S708); and RGG (M1-G168).

LAF-1 amino acid sequence (red, RGG domain; green, helicase domain):

1 MESNQSNNGGSGNAALNRGGRYVPPHLRGGDGG-AAAAASAGGDDRRGGAGGGGYRRGGGNSGGGG-GGGY

70 DRGYNDNRDDRDNRGGSGGYGRDRNYEDRGYNG-GGGGGGNRGYNNNRGGGGGGYNRQDRGDGGSSN-FSR

139 GGYNNRDEGSDNRGSGRSYNNDRRDNGGDGQN-TRWNNLDAPPSRGTSKWENRGARDERIEQELFSG-QLS

208 GINFDKYEEIPVEATGDDVPQPISLFSDLSLHEWIE-ENIKTAGYDRPTPVQKYSIPALQGGRDLMSCAQ

277 TGSGKTAAFLVPLVNAILQDGPDAVHRSVTSSGG-RKKQYPSALVLSPTRELSLQIFNESRKFAYRTPIT

346 SALLYGGRENYKDQIHKLRLGCHILIATPGRLIDV-MDQGLIGMEGCRYLVL**DEAD**RMLDMGFEPQIRQI

415 VECNRMPSKEERITAMFSATFPKEIQLLAQDFLKE-NYVFLAVGRVGSTSENIMQKIVWVEEDEKRSYLM

484 DLLDATGDSSLTLVFVETKRGASDLAYYLNRQNY-EVVTIHGDLKQFEREKHLDLFRTGTAPILVATAVA

553 ARGLDIPNVKHVINYDLPSDVDEYVHRIGRTGRV-GNVGLATSFFNDKNRNIARELMDLIVEANQELPDW

622 LEGMSGDMRSGGGYRGRGGRGNGQRFGGRDH-RYQGGSGNGGGGNGGGGGFGGGGQRSGGGGG-FQSGGGG

691 GRQQQQQQRAQPQQDWWS

LAF-1 E. coli expression and purification. BL21(DE3) cells transformed with the LAF-1 plasmid were grown until an OD of ∼0.4, induced with 500 μg/mL isopropyl β-D-1-thiogalactopyranoside, and grown overnight at 18 °C. Cells were pelleted and resuspended in lysis buffer [20 mM Tris·HCl, pH 7.4, 500 mM NaCl, 10 mM imidazole, 14 mM β-mercaptoethanol (ME), 10% (vol/vol) glycerol, and 1% Triton-X] containing 1 mg/mL lysozyme and a protease inhibitor mixture (Roche Diagnostics). Cells were lysed by sonication, and cellular debris was pelleted at 20,000 × *g* for 30 min. Cleared lysate was incubated with Ni-NTA agarose (Qiagen), washed well with Ni-Wash buffer [20 mM Tris·HCl, pH 7.4, 500 mM NaCl, 14 mM β-ME, 10% (vol/vol) glycerol, and 25 mM imidazole], and eluted with Ni-Elution buffer [20 mM Tris, pH 7.4, 500 mM NaCl, 14 mM β-ME, 10% (vol/vol) glycerol, and 250 mM imidazole].

Fractions were diluted 5× with room temperature heparin binding buffer [20 mM Tris, pH 7.4, 50 mM NaCl, 1% (vol/vol) glycerol, and 2 mM DTT] and loaded onto a HiTrap Heparin column (GE). Column was washed with heparin binding buffer and eluted in 20 mM Tris, pH 7.4, 1 M NaCl, 1% (vol/vol) glycerol, and 2 mM DTT. Glycerol was added to 10% (vol/vol), and aliquots were flash frozen in liquid nitrogen and stored at −80 °C.

For droplet experiments in vitro, individual LAF-1 frozen aliquots were thawed at room temperature, centrifuged at 14,000 × *g* for 2 min to remove any aggregated protein, and buffer exchanged (Amicon; 0.5 mL, 3–10k) into freshly made high salt buffer (20 mM Tris, pH 7.4, 1 M NaCl, and 1 mM DTT) to inhibit droplet formation. Protein solutions were subsequently mixed with varying volumes of no salt buffer (20 mM Tris, pH 7.4, and 1 mM DTT) to obtain desired protein/salt concentrations. All measurements were taken within 1 h of mixing with no salt buffer.

LAF-1::GFP insect cell purification. A codon-optimized LAF-1 ORF for bacterial and insect cell expression was synthesized by GeneScript USA and was cloned into a pOEM3G—a pOET vector derivative—using circular polymerase extension cloning (CPEC) (5). Specifically, pOEM3G and LAF-1 ORF were PCR amplified with primers that contained ∼30-nt complementary overhangs. Linear fragments were then combined in a second PCR, where complimentary sequences served as priming sites. The construct was amplified in

DH5α bacteria and cotransfected with bacmid DNA into SF+ insect cells. LAF-1::GFP was expressed in insect cells for 48 h. Afterward, cells were lysed, and protein was affinity-purified over nickel resin (NI-IDA; Invitrogen) and eluted with 100 mM imidazole, following standard protocols. Protein concentration was confirmed on Coomassie-stained gel and in a Bradford assay using BSA standard.

Phase Diagrams. Phase diagrams were generated by combining protein/salt mixtures into a coverslip/glass slide sealed with a rubber gasket (Grace BioLabs) and scoring yes/no for droplet formation based on DIC imaging using a 60× oil objected on an inverted Nikon microscope ∼1 h after mixing. To determine the saturation curve of LAF-1, protein/salt solutions were mixed and centrifuged for ∼3 h at 600 × *g* at 20 °C. The concentration in the bulk/dilute phase was measured directly using A280 and the Bradford assay (Biorad).

Fusion Experiments. Protein solution with a final NaCl concentration of 125 mM, total LAF-1 concentration of ∼3 μM, and ∼1% LAF-1_DyLight488 were placed into a chambered cover glass (Grace Bio-Labs) pretreated with 1% PF127 to minimize droplet wetting/surface interactions. Fusion events were monitored by 100-ms time lapses using a 100× objective on a spinning disk confocal. Fusion of two droplets of similar size was analyzed using Matlab according to previously published protocols (6).

Microrheology. Microrheology was generally performed as previously described (7). Briefly, green fluorescent microspheres (Invitrogen) of 0.5-μm radius with carboxyl surface chemistry were passivated with PEG-amine. PEGylated beads were added to low salt buffer before being mixed with a small volume of concentrated protein in high salt solution. As droplets form, fuse, and settle onto a PF127-treated cover slide, beads become randomly distributed within the droplet. Using a 40× air objective on a spinning disk confocal described above, measurements were taken at 500-ms time intervals for 500 s. Measurements were conducted for droplets ≈ 20 μm in diameter, and only beads residing several micrometers away from each interface were included in data analysis to avoid surface artifacts.

MSD data were fit (Fig. S2*A*) to the form $\mathrm{MSD}(\tau) = 4D\tau^{\alpha} + NF$, where α is the diffusive exponent, D is the diffusion coefficient, and NF is a constant representing the noise floor. NF was determined experimentally for beads stuck to a coverslip to be $\approx 2 \times 10^{-4}$ μm^2/s. We find $\alpha \approx 1$ for all measurements ($\alpha = 0.99 \pm 0.04$). Moreover, we find that bead diffusion scales with bead size, as predicted by the Stokes–Einstein relation (Fig. S2*B*): $D = k_B T/6\pi\eta a$, which for these equilibrium droplets can thus be used to extract a precise value for the droplet viscosity, η. MSD data are generated for individual beads within single droplets and averaged before extracting a viscosity. Reported viscosities are averages ± SD across multiple droplets.

FRAP. FRAP experiments were performed on a scanning confocal Nikon A1R inverted microscope. Recovery of a bleached spot of radius r = 1.5 μm inside droplets of diameter ≈ 10× the bleach radius were recorded. Intensity traces were corrected for photobleaching, normalized, and fit to an exponential function of the form

$$f(t) = A\left(1 - e^{-t/\tau}\right).$$

The recovery timescale, τ, was then used to determine the apparent diffusion coefficient $D_{app} \approx r^2/\tau$.

CD. CD spectra of LAF-1 proteins in high salt were collected on an Olis DSM 20. LAF-1 constructs (≈ 1 mg/mL) were prepared in high salt buffer. Data were collected at room temperature and consisted of averaging 10 individual spectra followed by buffer average subtraction.

RNA sample preparation. All RNA oligonucleotides substrates were purchased from IDT, either unlabeled or with either Cy3 or Cy5 dyes. The cRNA was modified with Cy3 (GE Healthcare) at its 5′ end. RNA constructs were annealed by mixing Cy3-labeled strand and Cy5-labeled complementary strand RNA at a molar ratio of 1:1 in T100 (10 mM Tris·HCl, pH 7.5, and 100 mM NaCl). The annealing reaction was performed by incubating at 65 °C for 5 min and then slowly cooling to room temperature for 3 h.

Single molecule FRET. Single molecule fluorescence experiments used quartz slides (Finkenbeiner) coated with PEG as described previously (8). Briefly, the slides and coverslips were cleaned with a combination of methanol, acetone, potassium hydroxide, and flame treatment. These slides were then coated with aminosilane followed by a mixture of 97.5% mPEG (m-PEG-5000; Laysan Bio) and 2.5% biotin PEG (biotin-PEG-5000; Laysan Bio). The annealed DNA molecules were immobilized on the PEG-passivated surface via a biotin–neutravidin interaction. All experiments and measurements were carried out at room temperature (22 ± 1 °C). Prism-type total internal reflection microscopy (TIRF) was used to acquire single molecule FRET. A 532-nm Nd:YAG laser was guided through a prism to generate an evanescent field of illumination. Data were recorded with a time resolution of 20–100 ms and analyzed with custom scripts written in interactive data language (IDL) to give fluorescence intensity time trajectories of individual molecules. Experiments were carried out in 50 mM Tris·HCl, pH 7.5, with the indicated NaCl concentration plus 1.0 mg/mL glucose oxidase, 0.2% glucose, ≈ 2 mM 6-hydroxy-2,5,7,8-tetramethylchromane-2-carboxylic (Trolox), and 0.01 mg/mL catalase.

Small molecule FRET data analysis. Basic data analysis was carried out by scripts written in Matlab, and the additional analysis software was coded in C++ and Matlab. FRET efficiency was calculated as the intensity of the acceptor channel divided by the sum of the donor and acceptor intensities after subtracting the background in the acquired microscope image. FRET histograms were generated using more than 10,000 individual molecules and were fitted to multiple Gaussian distributions using custom Matlab code by maximum likelihood estimation. Dwell times were collected by measuring the time that each molecule spends in a particular FRET state. Basic software for analyzing single-molecule FRET data is available for download from https://physics.illinois.edu/cplc/software/ and vbfret.sourceforge.net/.

1. Brenner S (1974) The genetics of Caenorhabditis elegans. *Genetics* 77(1):71–94.
2. Kamath RK, Martinez-Campos M, Zipperlen P, Fraser AG, Ahringer J (2001) Effectiveness of specific RNA-mediated interference through ingested double-stranded RNA in C. elegans. *Genome Biol* 2(1):1–10.
3. Kawasaki I, et al. (2004) The PGL family proteins associate with germ granules and function redundantly in Caenorhabditis elegans germline development. *Genetics* 167(2):645–661.
4. Mello CC, et al. (1996) The PIE-1 protein and germline specification in C. elegans embryos. *Nature* 382(6593):710–712.
5. Quan J, Tian J (2011) Circular polymerase extension cloning for high-throughput cloning of complex and combinatorial DNA libraries. *Nat Protoc* 6(2):242–251.
6. Brangwynne CP, Mitchison TJ, Hyman AA (2011) Active liquid-like behavior of nucleoli determines their size and shape in Xenopus laevis oocytes. *Proc Natl Acad Sci USA* 108(11):4334–4339.
7. Feric M, Brangwynne CP (2013) A nuclear F-actin scaffold stabilizes RNP droplets against gravity in large cells. *Nat Cell Biol* 15(10):1253–1259.
8. Roy R, Hohng S, Ha T (2008) A practical guide to single-molecule FRET. *Nat Methods* 5(6):507–516.

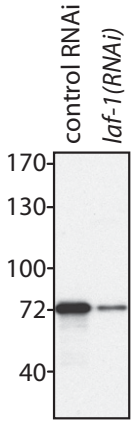

Fig. S1. Immunoblot of 25 gravid hermaphrodites per lane, probed with anti–LAF-1 monoclonal antibody.

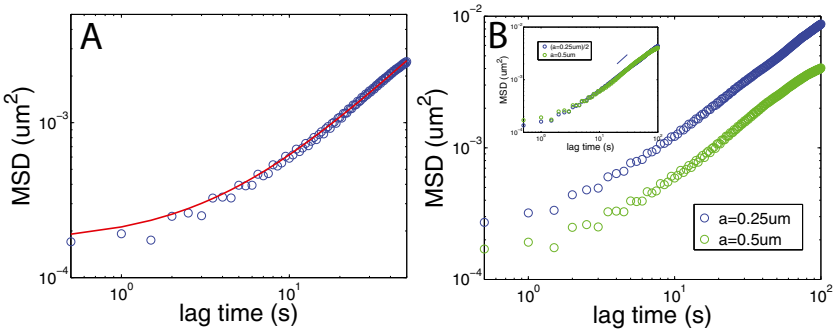

Fig. S2. Microrheology analysis. (*A*) A representative MSD dataset vs. time fit to the form $MSD(\tau) = 4D\tau^{\alpha} + NF$, where α is the diffusive exponent, D is the diffusion coefficient, and NF is a constant representing the noisefloor. NF was determined experimentally for beads stuck to a coverslip to be $\sim 2 \times 10^{-4}$ μm^2/s. Data plotted on a loglog plot. (*B*) MSD data for radius, $a = 5$ μm beads (green) and $a = 2.5$ μm beads (blue) diffusing inside LAF-1 droplets at 125 mM NaCl. (*Inset*) MSD data collapse when scaled by bead size.

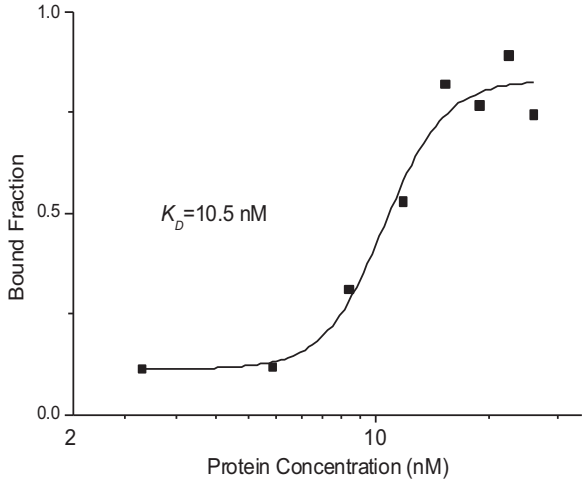

Fig. S3. LAF-1 RNA binding isotherm. Single molecule FRET traces were measured in 125 mM NaCl for LAF-1 concentrations up to ~20 nM, at which all of the RNA is bound. LAF-1 binding (in this concentration regime) results in a bimodal transition from an unbound RNA state (stable low FRET ~0.35) to a LAF-1–bound state (stable high FRET ~0.8). The increasing fraction of the LAF-1-bound high FRET values was calculated as a function of LAF-1 concentration. The resulting data collection was plotted with Origin 8.0 software using the Hill equation.

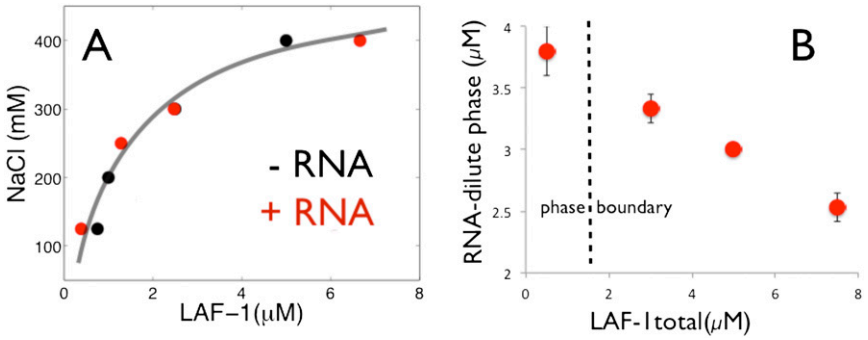

Fig. S4. RNA is recruited to droplets but does not shift the phase boundary. (*A*) Addition of 5 μM RNA has no effect on the phase diagram of LAF-1. (*B*) RNA concentration in the dilute phase vs. total LAF-1 concentration at 250 mM NaCl. Unlike LAF-1, which is in equilibrium with a constant saturation concentration in the dilute phase (Fig. 2*D*), the RNA concentration in the dilute phase decreases as total protein concentration increases. RNA concentration was directly measured using absorbance at A260 in the bulk phase after centrifugation of droplets.

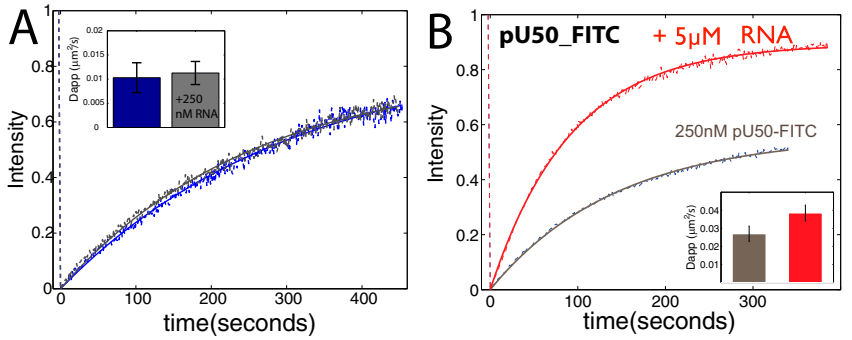

Fig. S5. (*A*) FRAP recovery for LAF-1 (fluorescently tagged) with 250 nM unlabeled RNA has little effect on LAF-1 diffusivity. Without RNA, timescale of recovery and apparent diffusion coefficient are 233 ± 61 s and 0.010 ± 0.003 μm^2/s, respectively, compared with 207 ± 40 s and 0.011 ± 0.002 μm^2/s for added 250 nM RNA. (*B*) The FRAP recovery timescale of low concentration of fluorescently labeled RNA (pU50-FITC) also decreases on addition of 5 μM pU50 RNA (red). (*Inset*) Calculated apparent diffusion coefficients.

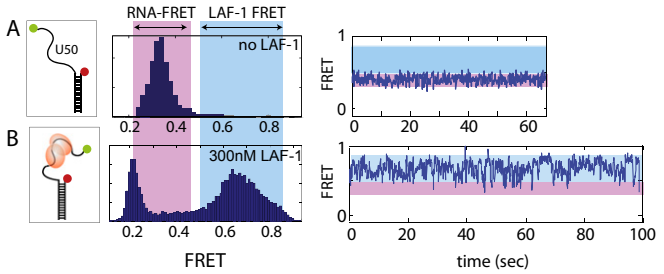

Fig. S6. FRET fluctuation induced by LAF-1 is not due to successive binding and unbinding of protein. (*A*) The FRET before LAF-1 binding is ~0.35 as represented by FRET histogram and single molecule FRET trace; FRET range is marked in purple bar. (*B*) The FRET fluctuation induced by LAF-1 near phase boundary condition is in the range of 0.5–0.8 as evidenced by FRET histogram and smFRET trace; FRET range is marked in light blue bar. The clear separation between the two FRET ranges indicates that FRET fluctuation is not due to successive LAF-1 binding and unbinding.

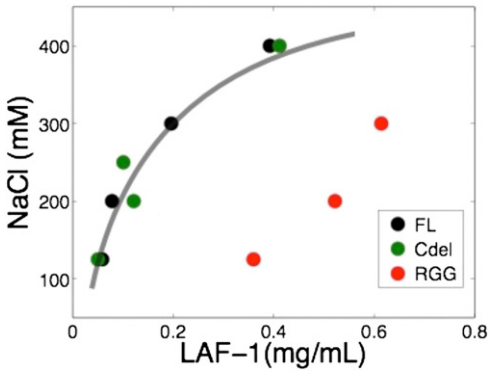

Fig. S7. Phase diagram LAF-1 truncations. Deletion of the C terminus (Cdel) (green) does not shift the phase boundary. The isolated RGG domain phase separates at significantly higher concentrations (red).

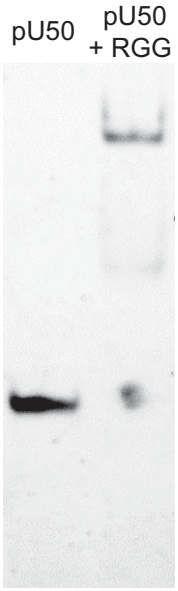

Fig. S8. The N-terminal RGG domain of LAF-1 binds RNA. EMSA gel of pU50 RNA (lane 1) and pU50 RNA incubated with 5 μM LAF1-RGG (lane 2) demonstrates RNA binding by the N-terminal RGG domain.